Atmospheric Environment 177 (2018) 54–63

Contents lists available at ScienceDirect

Atmospheric Environment

journal homepage: www.elsevier.com/locate/atmosenv

Analysis of multi-year near-surface ozone observations at the WMO/GAW "Concordia" station (75°06′S, 123°20′E, 3280 m a.s.l. – Antarctica)

Paolo Cristofanelli[a,*], Davide Putero[a], Paolo Bonasoni[a], Maurizio Busetto[a], Francescopiero Calzolari[a], Giuseppe Camporeale[d], Paolo Grigioni[b], Angelo Lupi[a], Boyan Petkov[a], Rita Traversi[c], Roberto Udisti[c], Vito Vitale[a]

[a] CNR–ISAC, National Research Council of Italy, Institute of Atmospheric Sciences and Climate, via Gobetti 101, 40129, Bologna, Italy
[b] ENEA, Laboratory for Observations and Analyses of Earth and Climate, C.R. Casaccia, 00123, S. Maria di Galeria (RM), Italy
[c] University of Florence, Dept. of Chemistry "Ugo Schiff", via della Lastruccia 3, 50019, Sesto Fiorentino (FI), Italy
[d] CNR-ISSIA, Institute of Intelligent Systems for Automation, via De Marini 6, 16149, Genova, Italy

ARTICLE INFO

Keywords:
Near-surface O_3
Antarctica
STT
Photochemistry

ABSTRACT

This work focuses on the near-surface O_3 variability over the eastern Antarctic Plateau. In particular, eight years (2006–2013) of continuous observations at the WMO/GAW contributing station "Concordia" (Dome C–DMC: 75°06′S, 123°20′E, 3280 m) are presented, in the framework of the Italian Antarctic Research Programme (PNRA). First, the characterization of seasonal and diurnal O_3 variability at DMC is provided. Then, for the period of highest data coverage (2008–2013), we investigated the role of specific atmospheric processes in affecting near-surface summer O_3 variability, when O_3 enhancement events (OEEs) are systematically observed at DMC (average monthly frequency peaking up to 60% in December). As deduced by a statistical selection methodology, these OEEs are affected by a significant interannual variability, both in their average O_3 values and in their frequency. To explain part of this variability, we analyzed OEEs as a function of specific atmospheric variables and processes: (i) total column of O_3 (TCO) and UV-A irradiance, (ii) long-range transport of air masses over the Antarctic Plateau (by Lagrangian back-trajectory analysis – LAGRANTO), (iii) occurrence of "deep" stratospheric intrusion events (by using the Lagrangian tool STLEFLUX). The overall near-surface O_3 variability at DMC is controlled by a day-to-day pattern, which strongly points towards a dominating influence of processes occurring at "synoptic" scales rather than "local" processes. Even if previous studies suggested an inverse relationship between OEEs and TCO, we found a slight tendency for the annual frequency of OEEs to be higher when TCO values are higher over DMC. The annual occurrence of OEEs at DMC seems related to the total time spent by air masses over the Antarctic plateau before their arrival to DMC, suggesting the accumulation of photochemically-produced O_3 during the transport, rather than a more efficient local production. Moreover, the identification of recent (i.e., 4-day old) stratospheric intrusion events by STEFLUX suggested only a minor influence (up to 3% of the period, in November) of "deep" events on the variability of near-surface summer O_3 at DMC.

1. Introduction

Tropospheric ozone (O_3) is a greenhouse gas and a driver for atmospheric oxidation capacity (Schultz et al., 2015). It is recognized as a "short-lived climate forcer" (SLCF, see UNEP & WMO, 2011), and its mean global concentration has at least doubled since the pre-industrial age. In contrast to other "well-mixed" greenhouse gases, its short atmospheric residence time, due to the high reactivity, still makes the quantification of O_3 long-term trends a challenging task (Cooper et al., 2014; Monks et al., 2015; Schultz et al., 2015).

Near-surface measurements carried out at remote locations like Antarctica provide the opportunity to investigate O_3 without a significant anthropogenic influence, thus giving information on O_3 background variability. However, O_3 in Antarctica presents some peculiarities that need to be accurately taken into account. Different processes have been recognized to affect O_3 in this region, including: intrusions of stratospheric air masses (Gruzdev & Sitnov, 1993; Roscoe, 2004), transport of air masses from lower latitudes (Murayama et al., 1992), and depletion processes involving reactive halogen atoms (Barrie et al., 1988; Roscoe et al., 2001). Moreover, summer episodes of sudden O_3 increases were observed within Antarctica interior (e.g., Crawford et al., 2001; Legrand et al., 2009), and at coastal sites affected by air

* Corresponding author.
E-mail address: p.cristofanelli@isac.cnr.it (P. Cristofanelli).

https://doi.org/10.1016/j.atmosenv.2018.01.007
Received 12 August 2017; Received in revised form 24 December 2017; Accepted 3 January 2018
Available online 08 January 2018

mass transport from the interior of the continent (e.g., Cristofanelli et al., 2011). These events were attributed to the photo-denitrification of the summer snowpack, resulting in NO_X emissions to the atmosphere and subsequent photochemical O_3 production (Jones et al., 1999, 2000). These processes are capable of driving the seasonality of near-surface O_3 over the Antarctic Plateau (Crawford et al., 2001; Legrand et al., 2009), thus potentially providing a significant input of O_3 to the whole Antarctic region (Legrand et al., 2016). Indeed, as shown in Cristofanelli et al. (2008) and Legrand et al. (2016), due to air mass transport, the photochemically-produced O_3 in the planetary boundary layer (PBL) over the Antarctic plateau can affect the O_3 variability also thousands of km far from the emission area. Previous investigations suggested that the O_3 production in the Antarctic PBL can be affected by several global/regional climate-related changes, i.e.: changes in UV fluxes due to total O_3 variability over Antarctica (Jones and Wolff, 2003; Frey et al., 2015), variability in long-range air mass transport patterns (Legrand et al., 2016), and depth of the continental mixing layer. Recently, Traversi et al. (2014, 2017) suggested that the variability of air mass transport from the stratosphere to the Antarctic plateau can affect nitrate content in the low troposphere and in the snowpack. Besides, the direct transport of air masses enriched in O_3 would represent another process by which stratosphere-to-troposphere transport (STT) events can potentially affect O_3 in the Antarctic troposphere.

In this work, we present the multi-year data series of near-surface O_3 at the Concordia World Meteorological Organization/Global Atmosphere Watch (WMO/GAW) contributing station (GAW ID: DMC) over January 2006–December 2013. The observations were carried out in the framework of different research projects funded by the Italian National Antarctic Programme (PNRA). This near-surface O_3 record was already successfully used to verify the MACC/MACC-2/CAMS-Copernicus global atmospheric composition forecast system (Wagner et al., 2015), and to investigate the variability of atmospheric Hg (Dommergue et al., 2012).

The main purpose of this paper is to provide a systematic assessment of the specific processes which affect near-surface summer O_3 inter-annual variability over an East Antarctic plateau area: (i) TCO and UV irradiance variability, (ii) synoptic-scale air mass transport within Antarctic interior, and (iii) "deep" STT transport. To reach these objectives, we analyzed the 2008–2013 measurement period, for which the highest data coverage was achieved at DMC and simultaneous irradiance and TCO measurements were available. A better understanding of the role played by these different processes in affecting the regional tropospheric O_3 variability would also help in evaluating the future response of Antarctic tropospheric O_3 to the ongoing global/regional changes. Moreover, since the mixing ratio of O_3 in the surface layer can also affect the chemical composition of the snowpack, a better knowledge of these processes would be very valuable for the interpretation of the ice core records retrieved at DMC (see, e.g., Helsen et al., 2007), which represent a reference for the investigation of past global climate and atmospheric composition variability.

2. Experimental and methodologies

2.1. Measurement site

The French-Italian "Concordia" station is located at Dome C (East Antarctic plateau, 75°06′S, 123°20′E, 3280 m a.s.l.); about 1200 km inland from the Ross Sea, and about 1100 km South of the coast of Adelie Land (Fig. 1). The station is part of the WMO/GAW network, and identified by the DMC acronym. In agreement with a previous experimental campaign (Petenko et al., 2004), the January 2006–December 2012 dataset showed that, during summer (November–January), the hourly temperature values ranged between −61.7 °C and −18.7 °C, while during winter (March–July), with permanent darkness, the temperature varied between −78.9 °C and −35.5 °C. In contrast to other Antarctic locations, and because of the flat orography and the lack of local drainage flows, DMC is not strongly affected by katabatic winds: historical wind records (Petenko et al., 2004; Argentini et al., 2003) and current observations (Fig. 2) showed a prevalent SW direction (average intensity of about 3 m s^{-1}, with the highest values around 20 m s^{-1}), without a clear annual cycle.

2.2. Near-surface O_3 measurements

During the measurement period (2006–2013), near-surface O_3 measurements were performed by using different UV absorption analyzers (Thermo Tei 49C, Thermo Tei 49i, and Dasibi 1108). The analyzers did not work in parallel, but they were changed and intercompared during the summer maintenance campaigns, usually occurring from December to January. To assure the intercomparability of measurements, before and after the installation at DMC, the O_3 analyzers were intercompared and calibrated against transfer O_3 calibrators (Dasibi 1003, from 2006 to 2010, and Thermo Tei49iPS, from 2010 to 2012), hosted at the WMO/GAW Mt. Cimone global station (Italy, GAW ID: CMN), and referred (2006–2008) to the national standard IMGC-O3SRP (hosted at the Italian National Institute for Metrological Research) and to the SRP#15 calibration scale (from 2008 onward), hosted at the WMO/GAW World Calibration Center for surface O_3, CO and CH_4 at EMPA (see Schultz et al., 2015). For the different analyzers, and over the whole measurement period, the total expanded (coverage factor $k = 2$) uncertainty has been assessed to be lower than 2 ppb. As a further QA/QC procedure, at DMC, every 24 h the instruments were challenged with a span value of about 100 ppb (obtained by an internal span source) and zero air obtained by flushing ambient air throughout a cartridge of activated charcoal with purafil©.

The O_3 observations were carried out at the "CARO–Clean Air Research Observatory" shelter, located 700 m SW with respect to the main base and upwind to the prevalent wind direction (Fig. 1). Air was collected from a 2 m stainless steel inlet placed on the roof of the shelter, at approximately 5 m above the snow surface. As indicated by Frey et al. (2015), the boundary layer height is lower than 10 m for a notable fraction of time (especially during the night) at DMC during summer. Pietroni et al. (2012), using the temperature profiles measured with a passive microwave radiometer, found a stable layer ranging from 10 to 150 m during winter and summer nights. Thus, it can be possible that, in some cases, our air inlet can be very close to the inversion layer, sampling air masses from the layer above the surface layer. The inlet was made inert to O_3 by passivation with UV exposure before the installation at DMC. A regular sampling flux was guaranteed by a turbo blower, while the sampling room was heated to avoid too low internal temperatures. The near-surface O_3 data were collected at 10-s intervals and stored as 1- and 30-min averages, together with the control parameters provided by the O_3 analyzer. Finally, to prevent and/or point out possible technical problems, the O_3 analyzer and the sampling line were regularly inspected by the personnel working in situ. This permitted to achieve a data coverage of 80% from January 2006 to December 2013. The first two years of observations (January 2006–December 2008) were characterized by a lower data coverage (57%), due to the occurrence of technical problems that prevented the execution of measurements during spring–winter periods. The near-surface O_3 record can be accessed from the WCDCGG web site (http://ds.data.jma.go.jp/gmd/wdcgg/cgi-bin/wdcgg/accessdata.cgi?index=DCC775S00-ISAC&orgn=ISAC&para=O3&select=inventory).

2.3. Surface meteorological measurements, total column of ozone (TCO) and UV irradiance

The meteorological variables used in this work were recorded by using an automated weather station (Vaisala, Mod. MILOS 520) located at about 100 m SW from the CARO shelter and managed by the "Osservatorio Meteo-Climatologico Antartico" (www.climantartide.it).

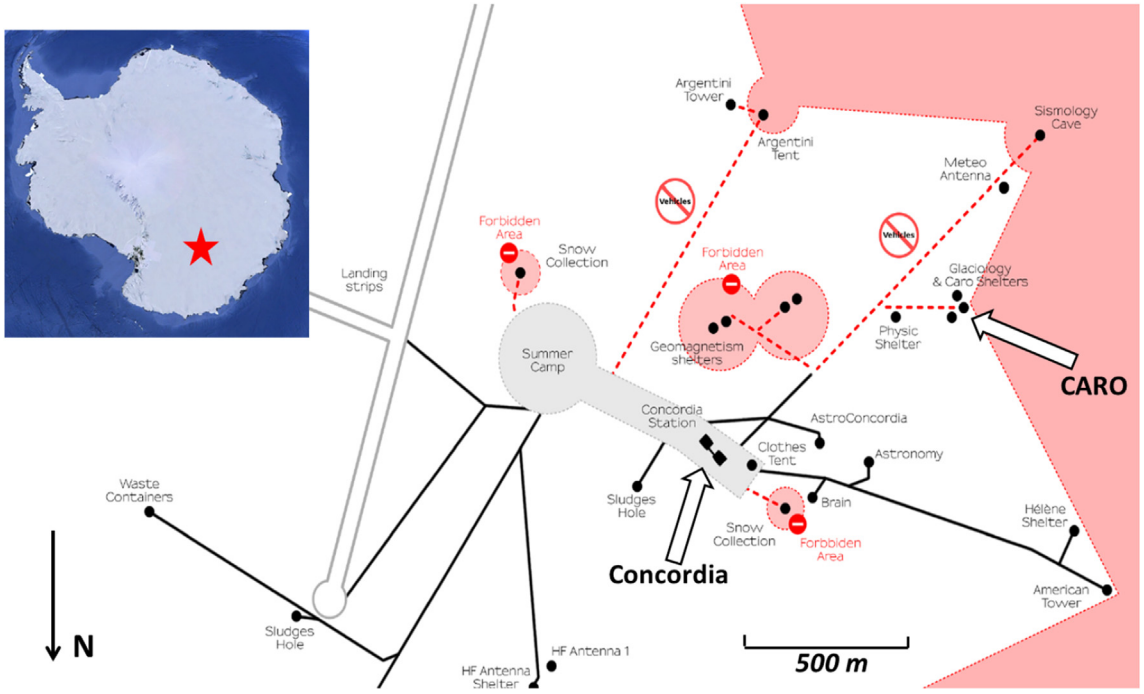

Fig. 1. Geographical location of Concordia station (insert: red star) and location of the CARO "Clean Air Research Observatory" (right) with respect to other station facilities: the "clean air" sectors (i.e., where anthropogenic activities are forbidden) are located from S–SE to N–NE (red shaded areas). (For interpretation of the references to colour in this figure legend, the reader is referred to the Web version of this article.)

The available instruments included a piezoelectric sensor for atmospheric pressure, a capacitor device for relative humidity, a thermocouple for air temperature, and a heated cup anemometer for wind speed and direction measurements. Meteorological data were recorded at 4 m above the snowpack for wind speed and direction, at 2 m for air temperature and relative humidity, and at 1.5 m for atmospheric pressure. Data were recorded every minute and validated on 1-h interval.

Since 2008, the total column of O_3 (TCO) is obtained from irradiance values observed by a narrowband filter radiometer UV-RAD, operating as part of the Baseline Surface Radiation Network (BSRN, see Ohmura et al., 1998). The UV-RAD is equipped with 7 spectral channels centered at peak wavelengths ranging between 0.300 and 0.364 μm, with each channel being defined by a set of pass-band filters determining an overall bandwidth of about 1 nm and transmittance varying between 12% and 27%. A comparison with OMI measurements showed an agreement on TCO measurements with mean uncertainty around ± 3% (Petkov et al., 2016).

2.4. LAGRANTO back-trajectories

To evaluate the synoptic-scale variability of the air masses reaching DMC, a set of 5-days back-trajectories starting at the measurement site was computed every 6 h (at 0:00, 6:00, 12:00 and 18:00 UTC), by using the Lagrangian analysis tool LAGRANTO (Wernli and Davies, 1997; Sprenger and Wernli, 2015). The model calculations were based on the ERA-Interim reanalysis dataset of the ECMWF (Dee et al., 2011). Each set comprised of 20 back-trajectories, with starting points shifted by ± 1° in latitude/longitude and in a vertical range of 50 hPa with respect to real DMC location, to partially compensate for uncertainties related to the absence of subgrid scale processes in LAGRANTO (e.g., convection and turbulent diffusion). The temporal resolution for the back-trajectories is one point every 2 h.

2.5. Identification of "deep" STT events

Stratosphere-to-troposphere transport (STT) events are well-known processes, able to influence tropospheric O_3 variability and near-surface O_3 within PBL of high-altitude regions (Škerlak et al., 2014). To assess the possible contribution of STT to near-surface O_3 variability in the DMC region, we identified the measurement periods possibly affected by "deep" STT events (i.e., stratospheric air masses transported down to the lower troposphere), by using the STEFLUX tool (Putero et al., 2016). STEFLUX is an algorithm for detecting the occurrence of STT events over specific target regions, by analyzing a pre-computed global stratosphere-to-troposphere exchange (STE) climatology produced by the IAC–ETH, Zurich (Škerlak et al., 2014). This climatology makes use of the ERA-Interim reanalysis dataset from the ECMWF (Dee et al., 2011), as well as a refined version of the well-developed Lagrangian methodology presented in Wernli and Bourqui (2002) for STE calculation. Basically, from a large set of global trajectories available each day, the ones that cross the tropopause (defined as the surface 2 pvu/380 K) within the first 24 h are retained. These are then extended backward and forward in time for additional 4 days, creating a 9-day trajectory. The application of a 3-D labelling algorithm is used to distinguish points of stratospheric and tropospheric nature, as well as potential anomalies (see Škerlak et al., 2014; for more details). STEFLUX detects the passage of these stratospheric trajectories within a 3-D target box on the region of interest. For this work, we set the top lid of the box at 590 hPa, and the following geographical boundaries: 74–77°S, and 122–125°E. A "deep" STT event at DMC was defined if at least 1 stratospheric trajectory crossed the 3-D target box.

To remove trajectories representing transient exchanges, a two-way minimum residence time criterion is applied in the Škerlak et al. (2014) STE climatology. This guarantees that only "robust" (i.e., not transient) STE events are considered by STEFLUX. A caveat for the Lagrangian approach on which STEFLUX is based is that it relies on trajectories calculated from resolved wind fields, which are characterized by a poor representation of subgrid scale convective and turbulent processes (Fueglistaler et al., 2004). Moreover, the trajectory calculations also do

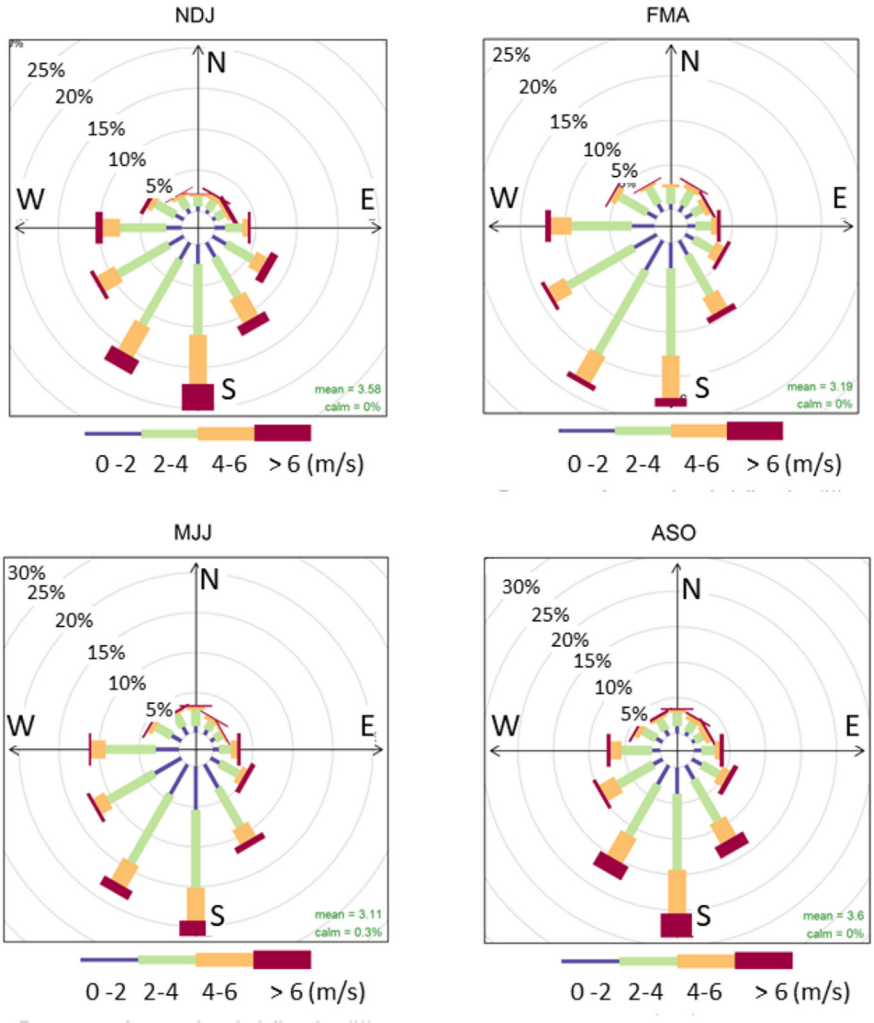

Fig. 2. Seasonal wind direction frequency analysis at DMC (January 2006–December 2013).

not account for stretching and mixing of the air parcels along the transport. Thus, STT trajectory-based studies provide a useful quantitative information only under the assumption that most of that exchange is associated with the large scale flow rather than subgrid processes. However, several studies (e.g., Trickl et al., 2016, and references therein) were successful (at least for the middle latitudes) in identifying stratospheric intrusions basing on kinematic trajectories, giving a certain confidence that the vertical winds in these analysis and reanalysis datasets are reasonable to diagnose STE.

3. Results

3.1. Near-surface O_3 variability

Fig. 3 shows the time series of mean daily O_3 values at DMC from January 2006 to December 2013. The seasonal cycles showed an increase from March to May, with a winter maximum (June–August) and a decline from September–October. For each year, the lowest monthly mean values were observed in February (ranging from 19.2 ppb to 21.0 ppb), while the highest monthly value were observed in July (during 2008–2012) and August (2013), with values ranging from 32.6 ppb to 35.0 ppb. This behavior (already pointed out by Legrand et al., 2009, 2016) clearly reflects the remoteness of Antarctica, with

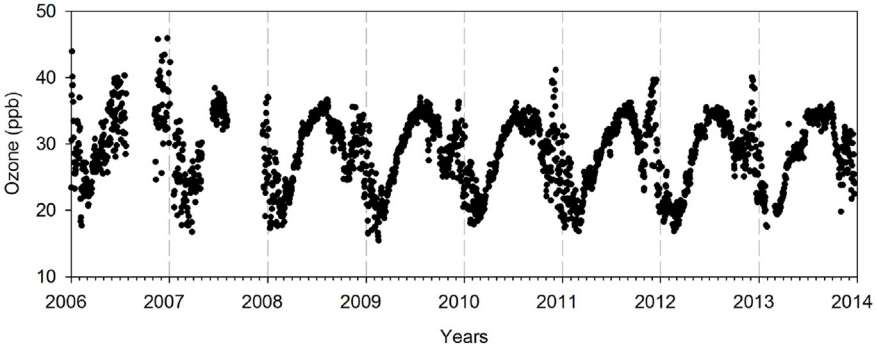

Fig. 3. Daily average O_3 values observed at DMC (January 2006–December 2013).

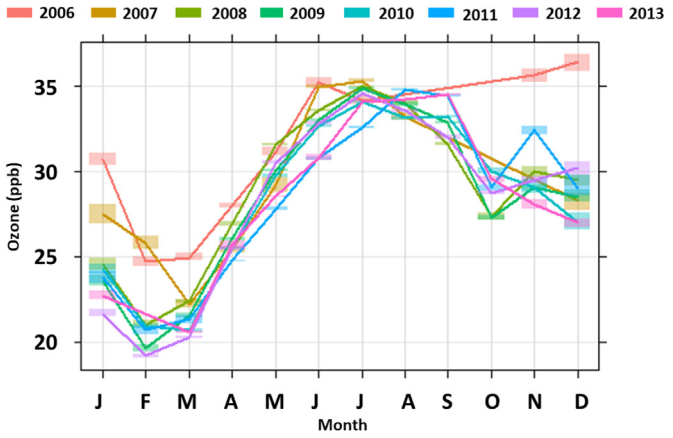

Fig. 4. Annual O_3 seasonal variations at DMC (2006–2013). For each month, the average mean value is reported together with the 95% confidence interval.

net O_3 accumulation during the darkness period and destruction when sunlight starts to reach the region, due to photolysis and chemical loss by OH and HO_2 in a low NO_X environment (Oltmans, 1981; Monks, 2000). However, in summer (i.e., November–January), episodes of sudden O_3 increase were systematically observed at DMC, with daily O_3 values approaching (or exceeding) those observed in winter. This feature appeared to be similar to what recorded at the other permanent continental station in Antarctica (the "Amundsen-Scott" station at South Pole), and can be attributed to the occurrence of O_3 enhancement events (OEEs) during the period November–January (Oltmans et al., 2008; Helmig et al., 2007). Despite their sporadic occurrence, as shown by the monthly O_3 values at DMC, these events are able to define the shape of seasonal near-surface O_3 cycle with monthly mean values in November and December exceeding 25 ppb (Fig. 4).

To characterize the typical monthly O_3 diurnal variations at DMC, we calculated the hourly deviations from the daily means for the period of investigation (Fig. 5). While no evident diurnal variations were recorded from March to October, a small reverse diurnal variation (~amplitude 0.7–1.0 ppb) was pointed out from November to February. For these months, the diurnal O_3 minima were observed around 6:00 UTC (i.e., 14:00 local time, LT), while the highest values were recorded around 12:00 UTC (i.e., 20:00 LT). To explain this behavior, near-surface wind speed was used as a proxy to evaluate the development of the convective boundary layer at DMC. Indeed, as reported in Argentini et al. (2005), during summer systematic wind speed diurnal cycles can be related to the presence of strong stability conditions (typically from 18:00 to 6:00 LT) and to the development of convective activity eroding the surface-based inversion and transferring momentum to the surface (typically from 7:00 to 17:00 LT). As reported in 5, the wind speed maximum (4–5 m s^{-1}) usually occurred before 14:00 LT, when the O_3 minima were observed from November to February. As also suggested by Legrand et al. (2016) and Mastrantonio et al. (1999), the diurnal development of the convective boundary layer favors the dilution of chemical species related to surface emissions. For near-surface O_3 this partially masks the role of local photochemical O_3 production related to NO_X release from snowpack. Based on the observed mixing ratios of NO and NO_2, and considering the loss reaction with OH, HO_2 and NO, Legrand et al. (2016), estimated a net averaged O_3 photochemical production of 0.3 ppb h^{-1} during summer light hours at DMC. Our observed O_3 average diurnal increase was 0.16 ppb h^{-1} from November to February, with significant variability of the 95% confidence interval (Table 1). In particular, the upper boundary of the 95th confidence level of the near-surface O_3 diurnal increase (in December and January) was well comparable with the estimated net photochemical O_3 production rates reported by Legrand et al. (2016) for specific case studies.

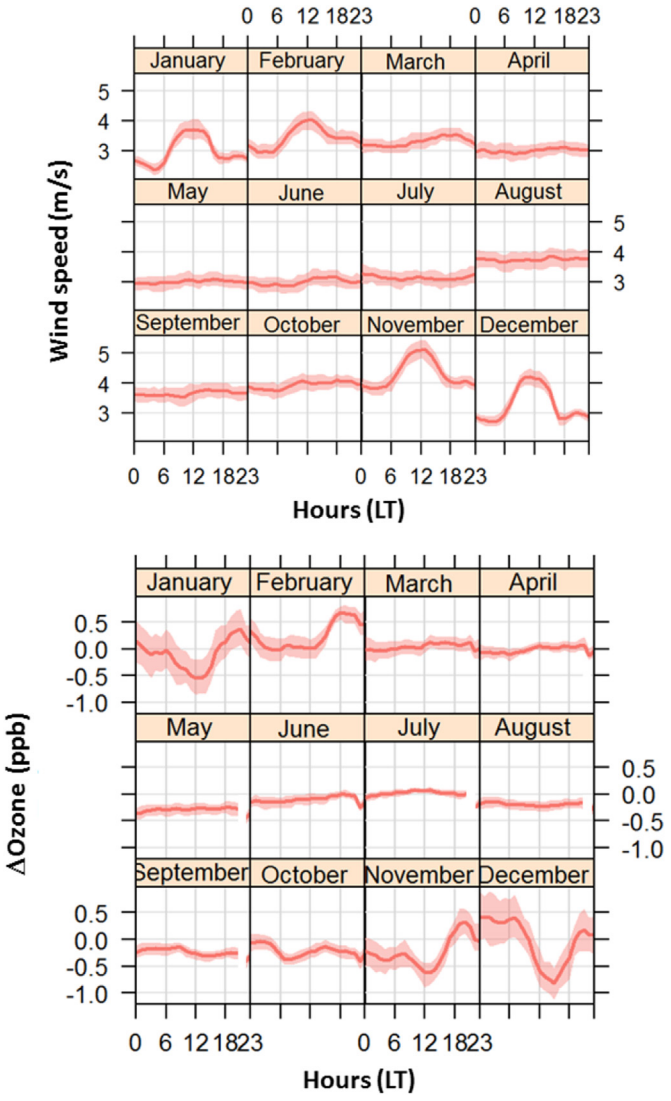

Fig. 5. Monthly wind speed (upper plate) and ΔO_3 (bottom plate) diurnal cycles at DMC (2006–2013). For each month, the average mean value is reported together with the 95% condense interval.

Table 1
Monthly average value of the 95th confidence level for the diurnal rate of near-surface O_3 increase at DMC.

Month	Upper limit (ppb h^{-1})	Lower limit (ppb h^{-1})
November	0.23	0.12
December	0.33	0.01
January	0.31	0.01
February	0.25	0.01

3.2. Analysis of summer "O_3 enhancement events" (OEEs)

3.2.1. Identification of OEEs

The analysis of OEEs was restricted to years 2008–2013, in which simultaneous measurements of UV irradiance and TCO values were available at DMC. Our method to select the days characterized by OEEs is based on a two-steps procedure. The first step consists in fitting the annual cycle of O_3 mean daily values with a sinusoidal curve. This represents an "undisturbed" O_3 annual cycle, not affected by the occurrence of summer O_3 events. In the second step, the probability density function (PDF) of the deviations from the sinusoidal fit is computed, considering all of the daily data. In the Supplementary Material, Fig. S1

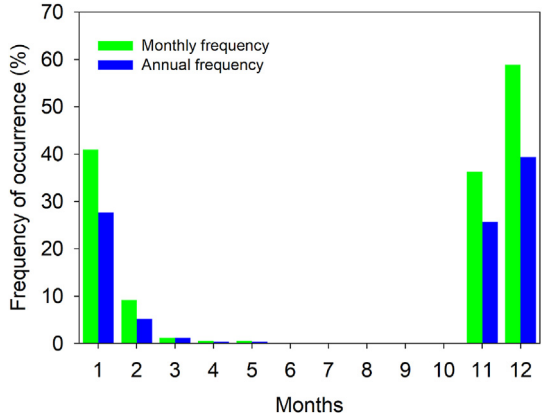

Fig. 6. Blue bars: averaged (over 2008–2013) distribution of the OEE occurrence among the different months of the year. Green bars: averaged frequency (over each single month) of OEEs. (For interpretation of the references to colour in this figure legend, the reader is referred to the Web version of this article.)

shows the sinusoidal curve superimposed to the time series of O_3 daily values, while Fig. S2 reports the PDF of the calculated deviations. Then, a Gaussian fit was applied to the obtained PDF. As reported by Giostra et al. (2011), the Gaussian distribution corresponds to a well-mixed state, given the hypothesis that instrumental errors and natural background variability follow a Gaussian distribution. The deviations from the Gaussian distribution (calculated by the Sigmaplot© statistical tool) would indicate observations affected by non-background variability. To obtain a threshold value for selecting non-background O_3 daily values possibly affected by "anomalous" O_3 enhancements, we calculated a further Gaussian fit for the PDF points falling above 1 σ (standard deviation) of the Gaussian PDF, and we considered the intersection between the two curves as our threshold value (i.e., 6 ppb). In total, 246 days (11.6% of the dataset) were selected as affected by anomalous OEEs: 25.7% in November, 39.3% in December, 27.7% in January and 5.1% in February (Fig. 6, blue bars).

Fig. 6 also reports (green bars), for each single month, the averaged occurrence of the anomalous events: the highest fraction of anomalous days was recorded in December, when more than half of the days were affected by the events, and slightly less values characterized November (35.5%) and October (37.1%); a non-negligible fraction of anomalous days was also recorded in February (7.6%).

Despite this clear annual cycle in the frequency of OEEs at DMC, we also observed significant interannual variability both in the O_3 mixing ratio and in the monthly frequency of events. In particular, the monthly frequency of OEEs ranged from 20% to 50%, as a function of the different years (Fig. 7).

To provide a quantification of the relative contribution of diurnal versus day-to-day O_3 variability during the OEEs, we compared the standard deviations of hourly and daily averaged datasets, as suggested by Chevalier et al. (2007). Indeed, the comparison between hourly and daily O_3 variability (expressed as standard deviations) allows to discriminate the relative contribution to the overall O_3 variability due to PBL photochemistry (and other processes occurring at diurnal scales) from processes occurring at longer time scales (i.e., weather variability, synoptic air mass transport, etc.). The variability based on hourly data presented a maximum in December (4.5 ppb) and a minimum in February (1.7 ppb): this clearly underpins the role played by diurnal-scale processes (i.e., PBL photochemistry and dynamics) in enhancing O_3 variability during summer (as suggested before). However, even in December, the ratio between daily and hourly standard deviations suggested that 84% of O_3 variability at DMC can be associated with processes occurring at longer temporal scales. With the purpose of attributing part of this variability, we analyzed several processes that, based on previous investigations, were indicated as likely to trigger the occurrence of summer O_3 enhancements over the Antarctic plateau. In particular, we investigated the possible role of: (i) TCO variability, (ii) synoptic-scale transport variability, and (iii) "deep" stratospheric intrusions events variability.

3.3. Possible influence of TCO variability and UV irradiance

Jones and Wolff (2003) proposed that TCO, and the related UV radiation variability at the surface, would affect near-surface O_3 by enhancing NO_X snow emissions and affecting O_3 photochemical production in the South Pole PBL over long time scales. For this reason, and to assess whether TCO variability could have a role in modulating the interannual O_3 summer concentrations at DMC, we analyzed TCO data observed at DMC. For the months on which the occurrence of OEEs was most likely (i.e., December–January), and for each different year (2008–2013), Fig. 7 shows the percentiles of hourly O_3 values during the OEEs (a–c), the OEEs frequency (d–f), together with percentiles of hourly TCO values (g–i) for the whole period of data availability. Although this analysis is somewhat qualitative and extended over a limited time period (6 years), we did not find clear anti-correlation between TCO and O_3 values during OEEs. On the other hand, by limiting the dataset to the days in which simultaneous data were available for all parameters (i.e., near-surface O_3 and irradiance measurements), we observed a positive (statistically significant at the 95% confidence level) correlation ($r^2 = 0.75$) between OEEs frequency and average TCO for November months (Fig. S3 in the Supplementary Material). A tendency for higher monthly occurrence of OEEs and higher monthly TCO can be also noticed for January (Fig. 7 and Fig. S3 in the Supplementary Material). This not systematic relationship between O_3 levels, OEEs frequency and TCO supports the finding by Frey et al. (2015) that the flux of NO_X in the surface atmospheric layer (and thus the related O_3 production) only depends on a secondary order from TCO variability.

Frey et al. (2015) pointed out that changes in surface downwelling UV irradiance lead to a quick response of mixing ratios and speciation of NO_X in ambient and firn air, as observed during a partial solar eclipse and during a shading experiment. However, they also stressed that, due to the presence of reservoir in the open pore space of the upper snowpack, the impact of changes in incident UV irradiance on the snow source, and thus NO_X flux and mixing ratios, can be observable on diurnal and seasonal timescales only. To assess whether the variability of UV-A irradiance could affect near-surface O_3 interannual variability throughout impact on NO_X flux from snowpack, we analyzed the monthly occurrences of OEEs and related near-surface O_3 values as a function of total dose of UV-A irradiance (315–400 nm) measured at DMC. UV-A has been considered since it covers the wavelength region of NO_3^- absorption (action spectrum maximum at 320 nm). As for TCO, it is difficult to find a clear relationship between monthly integrated UV-A dose and OEEs frequency, or average O_3 values during OEEs. A statistical significant (at the 90% confidence level) positive correlation for OEEs frequency and UV-A dose can be pointed out only for November ($r^2 = 0.45$), while a negative "tendency" ($r^2 = 0.60$) can be observed for January (Fig. S4 in the Supplementary Material).

3.4. Role of synoptic-scale air mass transport

As suggested by Legrand et al. (2016), the highest near-surface O_3 summer values were observed within air masses spending a significant fraction of time over the highest part of Antarctic plateau during the last 5 days before arriving at DMC. To investigate the possible influence of synoptic-scale air mass circulation to the occurrence of OEEs in November–January, we analyzed the 5-day LAGRANTO back-trajectories (Fig. 8). In particular, we used the potential source contribution function (PSCF) to calculate the conditional probabilities for identifying geographical regions related to the occurrence of OEEs at DMC (e.g. Hopke et al., 1995; Brattich et al., 2017). The residence time over each

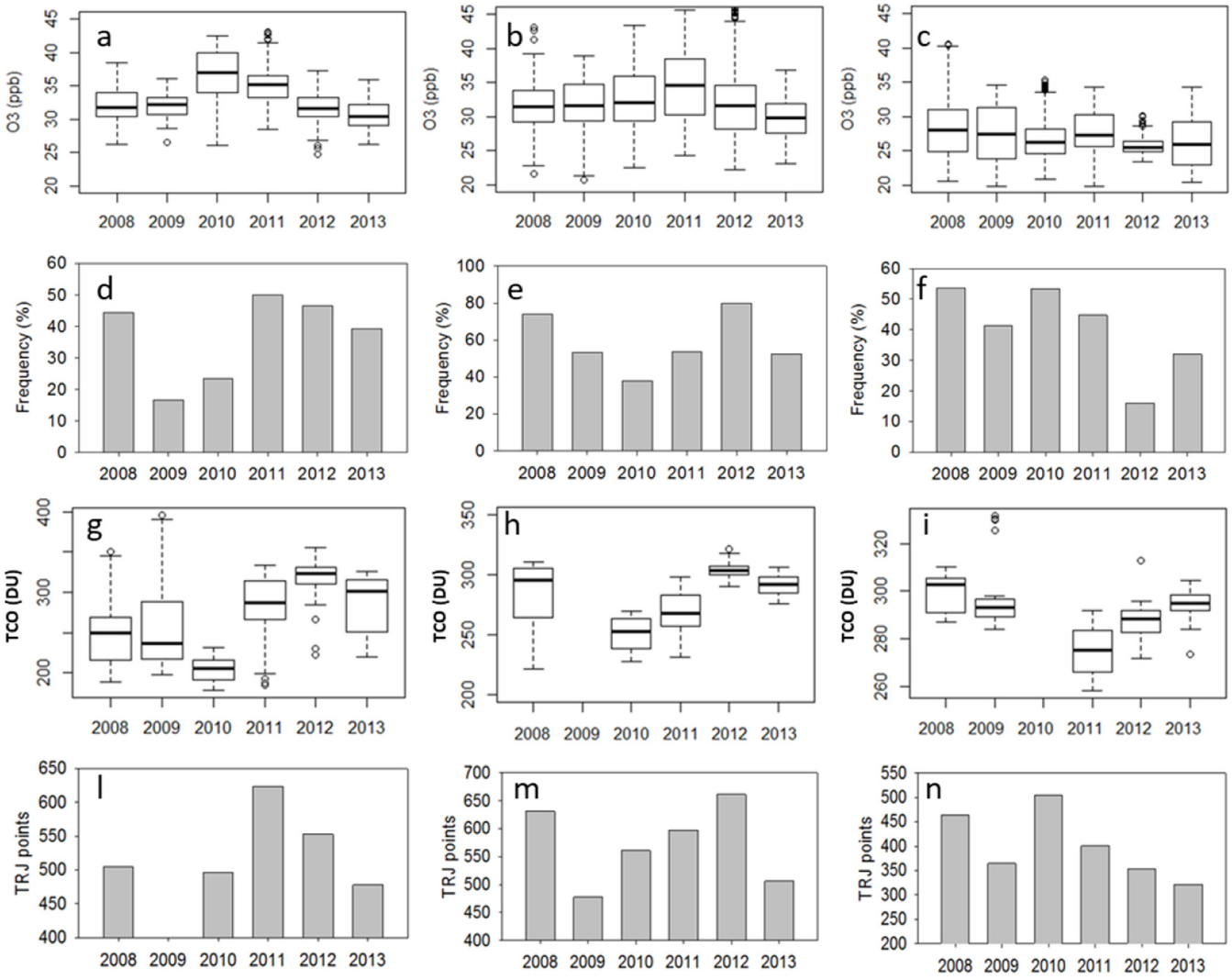

Fig. 7. For each month (November, December, January; each month is represented by a different column) we report the yearly percentiles (barbs and whiskers denote 10th, 25th, median, 75th and 90th percentiles, outliers are indicated as points) of hourly O_3 during the OEEs (a–c), the frequency of OEEs (d–f), the percentiles of hourly TCO (g–i) as well as the total number of hours that LAGRANTO back-trajectories spent over the Antarctic plateau (l–n).

i, j grid cell of the back-trajectory spatial domain (discretized into square grid cells of 1.0° × 1.0°) was calculated by selecting the number of trajectory endpoints falling within grid cell i, j over the whole measurement period ($n_{i,j}$). Then, in the same way, the residence time over each i, j grid cell corresponding to measurement period under OEEs was calculated ($m_{i,j}$). The PSCF for the grid cell i, j was then computed, according to Brattich et al. (2017):

$$PSCF = \frac{m_{i,j}}{n_{i,j}} = \frac{residence\ time\ of\ the\ air\ parcel\ during\ OEEs}{residence\ time\ of\ the\ air\ parcel} \quad (1)$$

To obtain a robust PSCF spatial field, only domain cells visited by at least 45 back-trajectories were retained. The results clearly highlight the connection between the occurrence of OEEs at DMC and air masses which traveled over the eastern Antarctic Plateau: PSCF values ranging from 40% to 50% were calculated for this region, while air masses advected from the western Plateau are characterized by very low PSCF values. Interestingly, regions with PSCF values exceeding 50% were pointed out not far from the coastline (around 70°S, 60°E) and over the Ocean (60°S, 145°E). With the purpose of attributing these features, we calculated the altitude (Z) above ground level (a.g.l.) of the back-trajectory points during OEEs. While back-trajectories moving over the eastern Plateau were characterized by Z values mostly below 500 m a.g.l. (which support the role of emissions from snowpack as a source of near-surface O_3), the regions with high PSCF values along the coastlines and over the ocean were characterized by relatively high Z (above 3000 m a.g.l.). This would indicate that these air masses traveled at "free tropospheric" altitudes from outside the continent to the Antarctic Plateau. As already suggested by Fiebig et al. (2014), elevated near-surface O_3 values in central Antarctica can be also related to the transport of free-tropospheric air mixed with aged pollution plumes originated at lower latitudes.

For each month, we computed the total time that air masses spent over the plateau (i.e., the area within the boundaries 90–70°S and 60–150°E) before reaching the measurement site (Fig. 7). Both considering the December–January period, as well as the single months, it is evident that an increase in the time spent by air masses over the plateau leads to an increase of enhancement event frequency at DMC. This correlation (Fig. 9) is statistically significant (at the 95% confidence level) for January ($r^2 = 0.62$) as well as for the whole December–January period ($r^2 = 0.69$). In agreement with Legrand et al. (2016), together with the analysis of hourly variability, this result points out that the synoptic-scale air mass transport plays a pivotal role in triggering the occurrence of enhancement near-surface O_3 events at DMC. If we (roughly) assume that the diurnal O_3 increase observed at DMC can be representative for the whole plateau, and if we assume that the air masses travelling over the plateau to DMC picked up "all" the

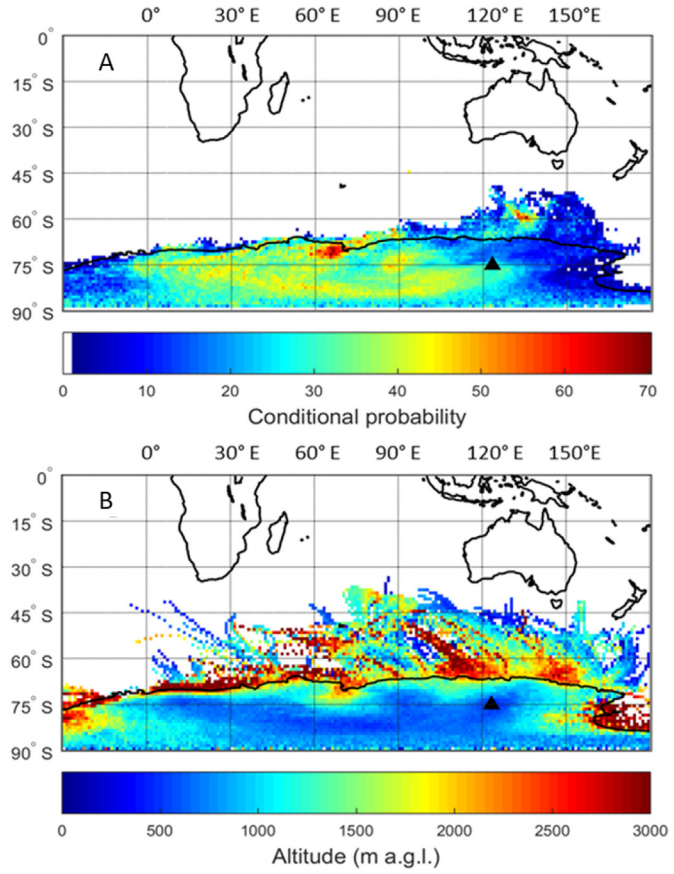

Fig. 8. Conditional probability field for the occurrence of OEEs at DMC (A) and average altitude (a.g.l.) of back-trajectories during OEEs (B). Please note that for the conditional probability field only cells visited by at least 45 back-trajectories were retained.

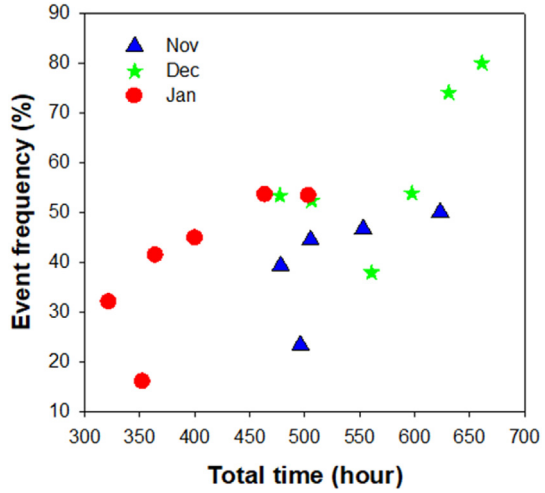

Fig. 9. Scatterplot of monthly total time spent by air masses over the plateau before the arrival at DMC versus monthly OEEs frequency for November (triangles), December (stars) and January (circles).

produced O_3 during a 5-day transport, an average O_3 accumulation on the air masses of about ~5 ppb can be calculated. This value is comparable with the day-to-day variability of near-surface O_3 observed at DMC, thus supporting the hypothesis that snowpack NO_X emissions may occur along the plateau on the daily scale. This would confirm that the synoptic-scale transport can favor the photochemical production and the accumulation of O_3 by air masses travelling over this region before their arrival to DMC.

3.5. Role of "deep" stratospheric transport

The possible role of air mass transport from the stratosphere in affecting the variability of near-surface O_3 and tropospheric air-chemistry in the Antarctic coastal region was investigated in previous studies (i.e., Murayama et al., 1992; Roscoe, 2004; Mihalikova and Kirkwood, 2013). By using a well-known Lagrangian approach based on the FLEXPART dispersion model, Stohl and Sodemann (2010) assessed that the direct influence of stratospheric air masses over the Antarctic Plateau is only about 2% per year. At the Troll station (72.0°S, 2.5°E, 1275 m a.s.l.), by analyzing in situ data from an atmospheric radar and ECMWF meteorological analysis, Mihalikova and Kirkwood (2013) estimated a significant higher occurrence of tropospheric folds, with a winter maximum (15–26% occurrence rate) and a summer minimum (6–7%). Traversi et al. (2014, 2017), described two possible case studies of stratospheric air mass transport at DMC, related to the advection of air masses linked to tropospheric folds, which occurred along the edge of the steep Antarctic coast, where air masses are orographically lifted up to 400 hPa. To provide a systematic assessment of the possible influence of "deep" STT events to the near-surface O_3 variability at DMC, we used the STEFLUX tool, proposed by Putero et al. (2016) as a relatively fast-computing Lagrangian algorithm to detect the occurrence of stratospheric intrusions over receptor regions in the troposphere, or in the boundary layer. Fig. 10 reports the average monthly frequency of "deep" stratospheric intrusions over the DMC 3-D target box (see Sect. 2.5). Although it is difficult to depict a clear seasonal cycle, due to the low frequency of "deep" STT events, our results are in agreement with Stohl and Sodemann (2010) (i.e., occurrence of STT lower than 2% on a monthly basis, without seasonal cycle). According to our STEFLUX outputs, the highest frequency of "deep" STT events was observed in November (2.8%). The frequency of occurrence of "deep" STT events identified by STEFLUX at DMC is about one order of magnitude lower than the occurrence of OEEs. Thus, a direct link of STT with OEEs interannual variability is unlikely. However, it should be noted that, according to Traversi et al. (2014, 2017), STT can represent a source of (stratospheric) nitrates for the Antarctic atmosphere, thus affecting also nitrate content in the snowpack through different processes (e.g., aerosol dry deposition, uptake of gaseous nitric acid by the uppermost snow layers). Hence, STT could indirectly affect near-surface O_3 variability by representing an input of nitrates that can be recycled by the snowpack and released as NO_X under sunlight conditions (Honrath et al., 2000), thus favoring the occurrence of OEEs.

4. Final remarks and conclusions

Measurements of O_3 mixing ratios carried out at the WMO/GAW Concordia station from 2006 to 2013 allowed to characterize near-

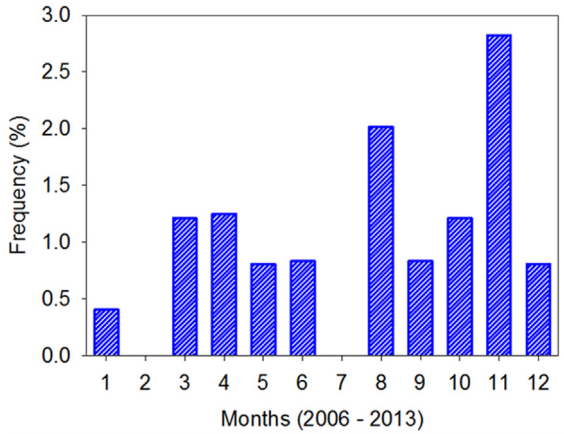

Fig. 10. Annual variation of "deep" STT events at DMC over the period 2006–2013, as obtained by STEFLUX.

surface O_3 variability over the eastern Antarctic Plateau, strengthening the availability of atmospheric composition observations in this remote region.

The systematic comparison of typical monthly diurnal cycles of O_3 with wind speed confirms the presence of a diurnal cycle that can be associated with photochemical production related to emissions of NO_X from nitrates in the snowpack and diurnal variability of the convective boundary layer. However, as deduced by the analysis of variability occurring at hourly and daily scales, the latter contribution dominated, suggesting that even during the photochemical "active" summer period, the synoptic transport somehow controls the overall O_3 variability (Neff et al., 2008). Since the occurrence of summer O_3 enhancement events (OEEs) showed significant interannual variability both in the monthly frequency and in the related O_3 mixing ratios, we analyzed a subset of specific processes able to influence them: (i) variability in TCO over the region, (ii) variability of synoptic-scale air-mass transport and (iii) occurrence of "deep" STT.

Jones and Wolff (2003) proposed that trends in downwelling UV irradiance due to TCO depletion at the South Pole could drive the summer net production of near-surface O_3 via changes in JNO_3^- and NO_X fluxes from the snowpack. In our data we did not find clear evidence for an impact of TCO and the related increase of UV surface fluxes with summer OEEs. This can be partially related also to the different location of DMC with respect to the South Pole. Indeed, the South Pole is characterized by modest but significant katabatic flows, implying a larger "catchment" area for surface air masses before arriving at the measurement site. Conversely, we found a positive tendency for increasing monthly TCO values and increasing occurrence of OEEs. Basing on 6 years of continuous O_3 and TCO observations, these results would support the fact (as already reported in Frey et al., 2015) that TCO is not the main driver for photochemical O_3 production in summer. At the moment, the positive relationship between TCO and OEEs occurrence for November is still not fully understood. We argue that this can be related to dynamical and synoptic-scale air mass circulations, which favor the advection of air masses rich in O_3 to the measurement site, under conditions of enhanced TCO. Indeed, the permanence of air masses over the continental plateau appears to be an important driver for the occurrence of OEEs at DMC. In agreement with Legrand et al. (2016), we found a rather clear relationship between the total time spent by air masses over the plateau and the interannual variability of the monthly occurrence of OEEs.

As deduced by the application of the STEFLUX tool, "deep" STT events only play a marginal role in steering the occurrence of OEEs at DMC via "direct" transport of O_3 from the stratosphere, or from the free troposphere, to the surface. It should be taken into account that, basing on the global STE climatology produced by Škerlak et al. (2014), STEFLUX is only able to consider relatively "young" (i.e., 4-day old) events. This can lead to an underestimation of the real influence of STT at DMC. However, as already suggested by Mihalikova and Kirkwood (2013), this Lagrangian tool based on ERA-Interim data may not have high enough spatial and vertical resolution to resolve the complex transport of stratospheric air masses down to the Antarctic plateau during STT. Moreover, Roscoe (2004) stated that stratospheric "material" transport can also occur via: (i) downward transport across the central Antarctic tropopause, (ii) subsidence in the stratosphere, and (iii) surface level suction to resupply katabatic winds draining the central Antarctic boundary layer. These processes cannot be captured by STEFLUX, and they cannot be reflected by "peak" events in the O_3 observations. Since it was proposed that STT can represent a source of nitrates for the Antarctic snowpack (thus possibly affecting summer NO_X re-emission and photochemical O_3 production), it is important to carry out further studies to better assess this process.

Acknowledgments

The authors are grateful to the atmospheric dynamics group at IAC–ETH (in particular Michael Sprenger and Heini Wernli) for help in calculating the backward trajectories. We recognize the importance of meteorological observations carried out at Concordia by ENEA throughout the "Osservatorio Meteo-Climatologico Antartico". The near-surface O_3 measurements presented in this work were carried out under PNRA Projects "DO3meCO2" and ABL-CLIMAT. The publication costs are supported by the PNRA 2014 A3-00091 "LTCPAA" Project. The present research was made possible by the joint French–Italian Concordia Program, which established and runs the permanent station Concordia at Dome-C. The authors are grateful to the Italian–French logistics team at CONCORDIA Station (IPEV–PNRA) for their kind assistance during the experimental campaign. We gratefully acknowledge the anonymous referee and Dr. H. K. Roscoe for their valuable comments.

Appendix A. Supplementary data

Supplementary data related to this article can be found at http://dx.doi.org/10.1016/j.atmosenv.2018.01.007.

References

Argentini, S., Mastrantonio, G., Viola, A., Nardino, M., Petenko, I., Sempreviva, A., 2003. PBL height behaviour at the plateau site of Dome C, Antarctica: sodar observations and numerical estimates. In: Proceedings of the 9th Workshop Italian Research on Antarctic Atmosphere, Rome, Italy, vol 80. pp. 13–26.

Argentini, S., Viola, A., Sempreviva, A.M., Petenko, I., 2005. Summer boundary-layer height at the plateau site of Dome'C, Antarctica. Boundary-Layer Meteorol. 115, 409–422. http://dx.doi.org/10.1007/s10546-004-5643-6. https://doi.org/10.1007/s10546-004-5643-6.

Barrie, L., Bottenheim, J., Schnell, R., Crutzen, P., Rasmussen, R., 1988. Ozone destruction and photochemical reactions at polar sunrise in the lower Arctic atmosphere. Nature 334, 138–141. http://dx.doi.org/10.1038/334138a0.

Brattich, E., Orza, J.A.G., Cristofanelli, P., Bonasoni, P., Tositti, L., 2017. Influence of stratospheric air masses on radiotracers and ozone over the central Mediterranean. J. Geophys. Res.: Atmosphere. http://dx.doi.org/10.1002/2017JD027036. (pp. n/a–n/a). https://doi.org/10.1002/2017JD027036.

Chevalier, A., Gheusi, F., Delmas, R., Ordóñez, C., Sarrat, C., Zbinden, R., Thouret, V., Athier, G., Cousin, J.-M., 2007. Influence of altitude on ozone levels and variability in the lower troposphere: a ground-based study for western Europe over the period 2001–2004. Atmos. Chem. Phys. 7, 4311–4326. http://dx.doi.org/10.5194/acp-7-4311-2007. https://www.atmos-chem-phys.net/7/4311/2007/.

Cooper, O.R., Parrish, D., Ziemke, J., Balashov, N., Cupeiro, M., Galbally, I., Gilge, S., Horowitz, L., Jensen, N., Lamarque, J.-F., Naik, V., Oltmans, S., Schwab, J., Shindell, D., Thompson, A., Thouret, V., Wang, Y., Zbinden, R., 2014. Global distribution and trends of tropospheric ozone: an observation-based review. Elementa: Sci. Anthrop. 2. http://doi.org/10.12952/journal.elementa.000029.

Crawford, J.H., Davis, D.D., Chen, G., Buhr, M., Oltmans, S., Weller, R., Mauldin, L., Eisele, F., Shetter, R., Lefer, B., Arimoto, R., Hogan, A., 2001. Evidence for photochemical production of ozone at the South Pole surface. Geophys. Res. Lett. 28, 3641–3644. http://dx.doi.org/10.1029/2001GL013055. https://doi.org/10.1029/2001GL013055.

Cristofanelli, P., Bonasoni, P., Calzolari, F., Bonaf, U., Lanconelli, C., Lupi, A., Trivellone, G., Vitale, V., Petkov, B., 2008. Analysis of near-surface ozone variations in terra nova bay, antarctica. Antarct. Sci. 20, 415–421. http://dx.doi.org/10.1017/S0954102008001028.

Cristofanelli, P., Calzolari, F., Bonafè, U., Lanconelli, C., Lupi, A., Busetto, M., Vitale, V., Colombo, T., Bonasoni, P., 2011. Five-year analysis of background carbon dioxide and ozone variations during summer seasons at the Mario Zucchelli station (Antarctica). Tellus B 63, 831–842. http://dx.doi.org/10.1111/j.1600-0889.2011.00576.x. https://doi.org/10.1111/j.1600-0889.2011.00576.x.

Dee, D.P., Uppala, S.M., Simmons, A.J., Berrisford, P., Poli, P., Kobayashi, S., Andrae, U., Balmaseda, M.A., Balsamo, G., Bauer, P., Bechtold, P., Beljaars, A.C.M., van de Berg, L., Bidlot, J., Bormann, N., Delsol, C., Dragani, R., Fuentes, M., Geer, A.J., Haimberger, L., Healy, S.B., Hersbach, H., Hólm, E.V., Isaksen, L., Kållberg, P., Köhler, M., Matricardi, M., McNally, A.P., Monge-Sanz, B.M., Morcrette, J.-J., Park, B.-K., Peubey, C., de Rosnay, P., Tavolato, C., Thépaut, J.-N., Vitart, F., 2011. The ERA-Interim reanalysis: configuration and performance of the data assimilation system. Q. J. Roy. Meteorol. Soc. 137, 553–597. http://dx.doi.org/10.1002/qj.828. https://doi.org/10.1002/qj.828.

Dommergue, A., Barret, M., Courteaud, J., Cristofanelli, P., Ferrari, C.P., Gallée, H., 2012. Dynamic recycling of gaseous elemental mercury in the boundary layer of the Antarctic Plateau. Atmos. Chem. Phys. 12, 11027–11036. http://dx.doi.org/10.5194/acp-12-11027-2012. https://www.atmos-chem-phys.net/12/11027/2012/.

Fiebig, M., Hirdman, D., Lunder, C.R., Ogren, J.A., Solberg, S., Stohl, A., Thompson, R.L., 2014. Annual cycle of Antarctic baseline aerosol: controlled by photooxidation-limited aerosol formation. Atmos. Chem. Phys. 14, 3083–3093. http://dx.doi.org/10.5194/acp-14-3083-2014. https://www.atmos-chem-phys.net/14/3083/2014/.

Frey, M.M., Roscoe, H.K., Kukui, A., Savarino, J., France, J.L., King, M.D., Legrand, M.,

Preunkert, S., 2015. Atmospheric nitrogen oxides (no and no_2) at dome c, east antarctica, during the opale campaign. Atmos. Chem. Phys. 15, 7859–7875. http://dx.doi.org/10.5194/acp-15-7859-2015. https://www.atmos-chem-phys.net/15/7859/2015/.

Fueglistaler, S., Wernli, H., Peter, T., 2004. Tropical troposphere-to-stratosphere transport inferred from trajectory calculations. J. Geophys. Res.: Atmosphere 109, D03108. http://dx.doi.org/10.1029/2003JD004069. n/a–n/a. https://doi.org/10.1029/2003JD004069.

Giostra, U., Furlani, F., Arduini, J., Cava, D., Manning, A., ODoherty, S., Reimann, S., Maione, M., 2011. The determination of a "regional" atmospheric background mixing ratio for anthropogenic greenhouse gases: a comparison of two independent methods. Atmos. Environ. 45, 7396–7405. http://www.sciencedirect.com/science/article/pii/S135223101100700X https://doi.org/10.1016/j.atmosenv.2011.06.076.

Gruzdev, A., Sitnov, S., 1993. Tropospheric ozone annual variation and possible troposphere-stratosphere coupling in the Arctic and Antarctic as derived from ozone soundings at Resolute and Amundsen-Scott stations. Tellus B 45, 89–98. https://doi.org/10.3402/tellusb.v45i2.15583.

Helmig, D., Oltmans, S.J., Carlson, D., Lamarque, J.-F., Jones, A., Labuschagne, C., Anlauf, K., Hayden, K., 2007. A review of surface ozone in the polar regions. Atmos. Environ. 41, 5138–5161. http://www.sciencedirect.com/science/article/pii/S1352231006012222 https://doi.org/10.1016/j.atmosenv.2006.09.053.

Helsen, M.M., Van de Wal, R.S.W., Van den Broeke, M.R., 2007. The isotopic composition of present-day Antarctic snow in a Lagrangian atmospheric simulation. J. Clim. 20, 739–756. http://dx.doi.org/10.1175/JCLI4027.1. https://doi.org/10.1175/JCLI4027.1.

Honrath, R.E., Peterson, M.C., Dziobak, M.P., Dibb, J.E., Arsenault, M.A., Green, S.A., 2000. Release of nox from sunlight-irradiated midlatitude snow. Geophys. Res. Lett. 27, 2237–2240. http://dx.doi.org/10.1029/1999GL011286. https://doi.org/10.1029/1999GL011286.

Hopke, P.K., Barrie, L.A., Li, S.-M., Cheng, M.-D., Li, C., Xie, Y., 1995. Possible sources and preferred pathways for biogenic and non-sea-salt sulfur for the high Arctic. J. Geophys. Res.: Atmosphere 100, 16595–16603. http://dx.doi.org/10.1029/95JD01712. https://doi.org/10.1029/95JD01712.

Jones, A.E., Wolff, E.W., 2003. An analysis of the oxidation potential of the South Pole boundary layer and the influence of stratospheric ozone depletion. J. Geophys. Res.: Atmosphere 108http://dx.doi.org/10.1029/2003JD003379. n/a–n/a. https://doi.org/10.1029/2003JD003379 4565.

Jones, A.E., Weller, R., Minikin, A., Wolff, E.W., Sturges, W.T., McIntyre, H.P., Leonard, S.R., Schrems, O., Bauguitte, S., 1999. Oxidized nitrogen chemistry and speciation in the Antarctic troposphere. J. Geophys. Res.: Atmosphere 104, 21355–21366. http://dx.doi.org/10.1029/1999JD900362. https://doi.org/10.1029/1999JD900362.

Jones, A.E., Weller, R., Wolff, E.W., Jacobi, H.-W., 2000. Speciation and rate of photochemical NO and NO_2 production in Antarctic snow. Geophys. Res. Lett. 27, 345–348. http://dx.doi.org/10.1029/1999GL010885. https://doi.org/10.1029/1999GL010885.

Legrand, M., Preunkert, S., Jourdain, B., Gallée, H., Goutail, F., Weller, R., Savarino, J., 2009. Year-round record of surface ozone at coastal (Dumont d'Urville) and inland (Concordia) sites in East Antarctica. J. Geophys. Res.: Atmosphere 114, D20306. http://dx.doi.org/10.1029/2008JD011667. n/a–n/a. https://doi.org/10.1029/2008JD011667.

Legrand, M., Preunkert, S., Savarino, J., Frey, M.M., Kukui, A., Helmig, D., Jourdain, B., Jones, A.E., Weller, R., Brough, N., Gallée, H., 2016. Inter-annual variability of surface ozone at coastal (Dumont d'Urville, 2004–2014) and inland (Concordia, 2007–2014) sites in East Antarctica. Atmos. Chem. Phys. 16, 8053–8069. http://dx.doi.org/10.5194/acp-16-8053-2016. https://www.atmos-chem-phys.net/16/8053/2016/.

Mastrantonio, G., Malvestuto, V., Argentini, S., Georgiadis, T., Viola, A., 1999. Evidence of a convective boundary layer developing on the Antarctic Plateau during the summer. Meteorol. Atmos. Phys. 71, 127–132. http://dx.doi.org/10.1007/s007030050050. https://doi.org/10.1007/s007030050050.

Mihalikova, M., Kirkwood, S., 2013. Tropopause fold occurrence rates over the Antarctic station Troll (72°S, 2.5°E). Ann. Geophys. 31, 591–598. http://dx.doi.org/10.5194/angeo-31-591-2013. https://www.ann-geophys.net/31/591/2013/.

Monks, P.S., 2000. A review of the observations and origins of the spring ozone maximum. Atmos. Environ. 34, 3545–3561. http://www.sciencedirect.com/science/article/pii/S1352231000001291 https://doi.org/10.1016/S1352-2310(00)00129-1.

Monks, P.S., Archibald, A.T., Colette, A., Cooper, O., Coyle, M., Derwent, R., Fowler, D., Granier, C., Law, K.S., Mills, G.E., Stevenson, D.S., Tarasova, O., Thouret, V., von Schneidemesser, E., Sommariva, R., Wild, O., Williams, M.L., 2015. Tropospheric ozone and its precursors from the urban to the global scale from air quality to short-lived climate forcer. Atmos. Chem. Phys. 15, 8889–8973. http://dx.doi.org/10.5194/acp-15-8889-2015. http://www.atmos-chem-phys.net/15/8889/2015/.

Murayama, S., Nakazawa, T., Tanaka, M., Aoki, S., Kawaguchi, S., 1992. Variations of tropospheric ozone concentration over Syowa Station, Antarctica. Tellus B 44, 262–272. http://dx.doi.org/10.1034/j.1600-0889.1992.t01-3-00004.x.

Neff, W., Perlwitz, J., Hoerling, M., 2008. Observational evidence for asymmetric changes in tropospheric heights over Antarctica on decadal time scales. Geophys. Res. Lett. 35, L18703. http://dx.doi.org/10.1029/2008GL035074. n/a–n/a. https://doi.org/10.1029/2008GL035074.

Ohmura, A., Gilgen, H., Hegner, H., Mller, G., Wild, M., Dutton, E.G., Forgan, B., Fröhlich, C., Philipona, R., Heimo, A., König-Langlo, G., McArthur, B., Pinker, R., Whitlock, C.H., Dehne, K., 1998. Baseline Surface Radiation Network (BSRN/WCRP): new precision radiometry for climate research. Bull. Am. Meteorol. Soc. 79, 2115–2136. http://dx.doi.org/10.1175/1520-0477(1998)079<2115:BSRNBW>2.0.CO;2. https://doi.org/10.1175/1520-0477(1998)079%3c2115:BSRNBW%3e2.0.CO;2.

Oltmans, S.J., 1981. Surface ozone measurements in clean air. J. Geophys. Res.: Oceans 86, 1174–1180. http://dx.doi.org/10.1029/JC086iC02p01174. https://doi.org/10.1029/JC086iC02p01174.

Oltmans, S.J., Johnson, B.J., Helmig, D., 2008. Episodes of high surface-ozone amounts at South Pole during summer and their impact on the long-term surface-ozone variation. Atmos. Environ. 42, 2804–2816. http://www.sciencedirect.com/science/article/pii/S1352231007000726 https://doi.org/10.1016/j.atmosenv.2007.01.020 Antarctic Tropospheric Chemistry Investigation (ANTCI) 2003.

Petenko, I., Argentini, S., Bolignano, A., Mastrantonio, G., Viola, A., 2004. Temporal and spatial variation of the summer convective boundary layer at the Antarctic plateau station of Dome C. In: Proceedings of the 10th Workshop Italian Research on Antarctic Atmosphere, Rome, Italy, vol. 89. pp. 199–215.

Petkov, B.H., Láska, K., Vitale, V., Lanconelli, C., Lupi, A., Mazzola, M., Budíková, M., 2016. Variability in solar irradiance observed at two contrasting Antarctic sites. Atmos. Res. 172–173, 126–135. http://www.sciencedirect.com/science/article/pii/S0169809516000168 https://doi.org/10.1016/j.atmosres.2016.01.005.

Pietroni, I., Argentini, S., Petenko, I., Sozzi, R., 2012. Measurements and parametrizations of the atmospheric boundary-layer height at dome c, antarctica. Boundary-Layer Meteorol. 143, 189–206. http://dx.doi.org/10.1007/s10546-011-9675-4. https://doi.org/10.1007/s10546-011-9675-4.

Putero, D., Cristofanelli, P., Sprenger, M., Škerlak, B., Tositti, L., Bonasoni, P., 2016. STEFLUX, a tool for investigating stratospheric intrusions: application to two WMO/GAW global stations. Atmos. Chem. Phys. 16, 14203–14217. http://dx.doi.org/10.5194/acp-16-14203-2016. https://www.atmos-chem-phys.net/16/14203/2016/.

Roscoe, H., 2004. Possible descent across the tropopause in antarctic winter. Adv. Space Res. 33, 1048–1052. http://www.sciencedirect.com/science/article/pii/S0273117703005878 https://doi.org/10.1016/S0273-1177(03)00587-8 (Climate Change Processes in the Stratosphere, Earth-Atmosphere-Ocean Systems, and Oceanographic Processes from Satellite Data).

Roscoe, H.K., Kreher, K., Friess, U., 2001. Ozone loss episodes in the free Antarctic troposphere, suggesting a possible climate feedback. Geophys. Res. Lett. 28, 2911–2914. http://dx.doi.org/10.1029/2000GL012583. https://doi.org/10.1029/2000GL012583.

Schultz, M.G., Akimoto, H., Bottenheim, J., Buchmann, B., Galbally, I.E., Gilge, S., Helmig, D., Koide, H., Lewis, A.C., Novelli, P.C., Plass-Dülmer, C., Ryerson, T.B., Steinbacher, M., Steinbrecher, R., Tarasova, O., Tørseth, K., Thouret, V., Zellweger, C., 2015. The Global Atmosphere Watch reactive gases measurement network. Elementa: Sci. Anthrop. 3. http://doi.org/10.12952/journal.elementa.000067.

Škerlak, B., Sprenger, M., Wernli, H., 2014. A global climatology of stratosphere–troposphere exchange using the ERA-Interim data set from 1979 to 2011. Atmos. Chem. Phys. 14, 913–937. http://dx.doi.org/10.5194/acp-14-913-2014. https://www.atmos-chem-phys.net/14/913/2014/.

Sprenger, M., Wernli, H., 2015. The LAGRANTO Lagrangian analysis tool – version 2.0. Geosci. Model Dev. (GMD) 8, 2569–2586. http://dx.doi.org/10.5194/gmd-8-2569-2015. https://www.geosci-model-dev.net/8/2569/2015/.

Stohl, A., Sodemann, H., 2010. Characteristics of atmospheric transport into the Antarctic troposphere. J. Geophys. Res.: Atmosphere 115, D02305. http://dx.doi.org/10.1029/2009JD012536. n/a–n/a. https://doi.org/10.1029/2009JD012536.

Traversi, R., Udisti, R., Frosini, D., Becagli, S., Ciardini, V., Funke, B., Lanconelli, C., Petkov, B., Scarchilli, C., Severi, M., Vitale, V., 2014. Insights on nitrate sources at Dome C (East Antarctic Plateau) from multi-year aerosol and snow records. Tellus B 66, 22550. http://dx.doi.org/10.3402/tellusb.v66.22550. https://doi.org/10.3402/tellusb.v66.22550.

Traversi, R., Becagli, S., Brogioni, M., Caiazzo, L., Ciardini, V., Giardi, F., Legrand, M., Macelloni, G., Petkov, B., Preunkert, S., Scarchilli, C., Severi, M., Vitale, V., Udisti, R., 2017. Multi-year record of atmospheric and snow surface nitrate in the central Antarctic plateau. Chemosphere 172, 341–354. http://www.sciencedirect.com/science/article/pii/S0045653516318872 https://doi.org/10.1016/j.chemosphere.2016.12.143.

Trickl, T., Vogelmann, H., Fix, A., Schäfler, A., Wirth, M., Calpini, B., Levrat, G., Romanens, G., Apituley, A., Wilson, K.M., Begbie, R., Reichardt, J., Vömel, H., Sprenger, M., 2016. How stratospheric are deep stratospheric intrusions? luami 2008. Atmos. Chem. Phys. 16, 8791–8815. http://dx.doi.org/10.5194/acp-16-8791-2016. https://www.atmos-chem-phys.net/16/8791/2016/.

UNEP, WMO, 2011. Integrated Assessment of Black Carbon and Tropospheric Ozone.

Wagner, A., Blechschmidt, A.-M., Bouarar, I., Brunke, E.-G., Clerbaux, C., Cupeiro, M., Cristofanelli, P., Eskes, H., Flemming, J., Flentje, H., George, M., Gilge, S., Hilboll, A., Inness, A., Kapsomenakis, J., Richter, A., Ries, L., Spangl, W., Stein, O., Weller, R., Zerefos, C., 2015. Evaluation of the MACC operational forecast system – potential and challenges of global near-real-time modelling with respect to reactive gases in the troposphere. Atmos. Chem. Phys. 15, 14005–14030. http://dx.doi.org/10.5194/acp-15-14005-2015. https://www.atmos-chem-phys.net/15/14005/2015/.

Wernli, H., Bourqui, M., 2002. A Lagrangian "1-year climatology" of (deep) cross-tropopause exchange in the extratropical Northern Hemisphere. J. Geophys. Res.: Atmosphere 107http://dx.doi.org/10.1029/2001JD000812. ACL 13–1–ACL 13–16. https://doi.org/10.1029/2001JD000812.

Wernli, B.H., Davies, H.C., 1997. A Lagrangian-based analysis of extratropical cyclones. I: the method and some applications. Q. J. Roy. Meteorol. Soc. 123, 467–489. http://dx.doi.org/10.1002/qj.49712353811.